Research Square

Preprints are preliminary reports that have not undergone peer review.
They should not be considered conclusive, used to inform clinical practice,
or referenced by the media as validated information.

Preparation and properties of high-dielectric-constant, heat-resistant boroxine-containing segmented copolyimides

Shengjie Ge
Hefei University of Technology
Xiang Zhang
Hefei University of Technology
Fengmei Ren
renfm@hfut.edu.cn
Hefei University of Technology
Haihong Ma
Hefei University of Technology
Zhengfa Zhou
Hefei University of Technology
Weibing Xu
Hefei University of Technology

Research Article

Keywords: Polyimide, Heat resistance, High dielectric constant, Boroxine containing, Soft-hard segmented

Posted Date: November 16th, 2026

DOI: https://doi.org/10.21203/rs.3.rs-11102148/v1

License: This work is licensed under a Creative Commons Attribution 4.0 International License.
Read Full License

Additional Declarations: No competing interests reported.

Preparation and properties of high-dielectric-constant, heat-resistant boroxine-containing segmented copolyimides

Shengjie Ge[1], Xiang Zhang[1], Fengmei Ren[1*], Haihong Ma[1], Zhengfa Zhou[1], Weibing Xu[1].

[1]*School of Chemistry and Chemical Engineering, Hefei University of Technology, 230009 Hefei, China*

Abstract

Polyimide (PI) is widely used as dielectric materials in electronic devices and power systems because of its excellent heat resistance and mechanical stability. However, the intrinsically low dielectric constant of conventional PI limits its practical application in high-energy-density dielectric capacitors. In this study, triaminocycloboroxane (TABO) was first synthesized via dehydration condensation of 3-aminophenylboronic acid (3-ABBA). TABO was then reacted with 3,3',4,4'-biphenyltetracarboxylic dianhydride (BPDA) via an amine-anhydride ring-opening addition reaction to prepare a boron-containing hard-segment polyamic acid prepolymer, which designated as PAA-a. Separately, a soft-segment polyamic acid prepolymer, designated as PAA-b, was synthesized by reacting 4,4'-diaminodiphenyl ether (ODA) with 4,4'-oxydiphthalic dianhydride (ODPA) through the same method. PAA-a and PAA-b were coupled through ring-opening polyaddition to form a soft-hard segmented polyamic acid (PAA). The resulting PAA was cast into films, dried, and thermally imidized to obtain boroxine-containing PI films. The effects of the reactant ratio on soft-hard segmented structure, dielectric, thermal, wetting and mechanical properties of the PI films were studied. The results showed that raising the molar ratio of TABO to ODA, the hard-segment content of as-prepared PI films increased, and the dielectric and thermal

* Address correspondence to E-mail: renfm@hfut.edu.cn

properties were improved. When the molar ratio of TABO to ODA was 2:27, the PI film exhibited a high dielectric constant of 5.08 at 100 kHz and a maximum decomposition rate temperature of 630 °C. These results demonstrate its potential as a high dielectric material for high-energy-density capacitors.

Keywords

Polyimide; Heat resistance; High dielectric constant; Boroxine containing; Soft-hard segmented

1 Introduction

With the rapid development of 5G communication, new energy vehicles, aerospace and other fields, the demand for high-performance dielectric materials is increasingly urgent. Applications such as high-energy storage density capacitors, extreme-environment resistant insulation coatings and high-power density packaging systems require materials with excellent dielectric properties, thermal stability and mechanical properties. Although traditional polymer dielectric materials, such as biaxially oriented polypropylene (BOPP)[1] and polyvinylidene fluoride (PVDF)[2], have low dielectric loss, their heat resistance and dielectric constant are difficult to meet the demands of high-temperature, high-dielectric-constant. Polyimide (PI) has become an indispensable dielectric material in the microelectronic industry owing to its excellent high temperature resistance, mechanical strength and dielectric stability, arising from the synergistic effect of rigid aromatic ring and flexible ether bonds in the molecular chain[3]. However, the intrinsically moderate dielectric constant of conventional PI, typically ranging f rom 2.5 to 3.5 at 100 kHz, limits its use in energy storage equipment and other applications re

quiring high permittivity.

The introduction of inorganic fillers with high dielectric constant can improve the dielectric properties of PI by enhancing the interface polarization. Ren et al.[4] successfully prepared the core-shell structure of Al_2O_3@ZrO_2 nano filler by coating ZrO_2 with amorphous Al_2O_3 nano layer by sol-gel method. The polyetherimide (PEI) composites filled with the core–shell structured nanoparticles composed of ZrO_2 core and Al_2O_3, the thickness of amorphous Al_2O_3 nano layer was adjusted according to different reaction time. The composites achieved a dielectric constant of 3.89 at 1kHz, 20% higher than that of the pure PEI, while maintaining a low dielectric loss of 0.004. Xu et al.[5] prepared black phosphorus (BP) nanosheets by liquid-phase exfoliation method. The dried BP nanosheets were dispersed in N-methylpyrrolidone, and BP-PI composites were prepared by in-situ polymerization. The composite film achieved a dielectric constant of 8.65 with a dielectric loss of 0.02 at 100 Hz. However, the introduction of inorganic fillers leads to filler agglomeration, interface defects and uneven dispersion, resulting in a decline in mechanical strength of the PI matrix and deterioration of processing performance. Furthermore, the dielectric loss increases and the breakdown strength decreases due to interface polarization and electric field distortion.

An alternative approach is chemical modification, in which highly polar groups or structural units are introduced into the backbone of the PI to generate strong dipole moment and enhance orientational polarization[6]. Tong et al.[7] synthesized a series of novel sulfonyl-containing polyimide dielectrics via condensation polymerization of two monomer pairs—one bearing highly polar sulfonyl groups and the other incorporating flexible ether linkages. The as-prepared PI with sulfonyl group in diamine moiety and para-para linkage exhibits a high

dielectric constant of 5.98 at 1 kHz and a superior glass transition temperature (*Tg*) of 304 ℃. Zhu et al.[8] first synthesized diamine containing high dipole moment cyano group, and then condensed and polymerized with five different dianhydride to prepare modified polyimide. The strong intermolecular force of cyano group enable the modified PI to achieve a *Tg* of 325 ℃. In terms of dielectric properties, the high orientation polarization of cyano group and close chain stacking synergism make the dielectric constant of modified PI reached 4.8 at 1 kHz. Chen et al.[9] first synthesized carboxylic acid terminated copper phthalocyanine oligomer (o-CuPc) by solution method, and then thermally dehydrated o-CuPc at 200 ℃ in vacuum to form anhydride terminated copper phthalocyanine anhydride oligomer (o-CuPcA). Then it reacts with dianhydride diamine to form polyamic acid (PAA), and finally it is thermally imidized at 300 ℃ to form copolymer film. The resulting film presented excellent thermal stability, with a 5% weight-loss temperature ($T_{5\%}$) of 500 ℃, and its dielectric constant reached 42.4 at 100 Hz. However, the dielectric constant of such copolymer remains insufficient above 100 kHz, and its synthesis of chemical modification is inherently complex, with a risk of by-product formation. In addition, increased rigidity and hygroscopicity from chemical modification compromise processability, stability, and mechanical properties[10].

Boron atoms have low electronegativity and form highly polar boron-oxygen bonds with oxygen atoms. These bonds possess have large dipole moments, which enhance the polarization ability of a material under an electric field, thus improving the dielectric constant of materials[11]. Moreover, the B-O bond dissociation energy, reported at approximately 536 kJ/mol, contributes to enhanced thermal stability of the polymer network. Wu et al. [12]significantly improved the high temperature resistance of phenolic aerogels by introducing

boric acid. At high temperatures, the B-O bond not only enhanced the thermal stability of the molecular skeleton, but also oxidized in the air to form a dense B_2O_3 protective layer, blocking oxygen penetration and inhibiting deep oxidation, which increased the mass residue rate from 36.5% to 54.9% at 1000 ℃. Wang et al.[13] reported the grafting of 4-formylphenylboronic acid onto amino-modified functionalized polydimethylsiloxane through the reaction between the formyl and amino groups. The resulting boronic acid groups subsequently underwent dehydration condensation to form a boroxine cross-linked structure, which enhanced the thermal stability of the material and raised the $T_{5\%}$ to 345 °C.

At present, research on the dielectric properties of boroxine-modified polymers remains scarce. In this study, triaminocycloboroxane (TABO) was synthesized via dehydration and condensation of 3-aminophenylboronic acid (3-ABBA). By varying the molar ratio of TABO to 4,4'-diaminodiphenyl ether (ODA), a series of boroxine-containing PAAs were successfully synthesized via ring-opening polyaddition. Subsequent casting and thermal imidization yielded a series of boroxine-containing PI films. When the molar ratio of TABO to ODA was 2:27, the resulting PI film exhibited excellent dielectric and thermal properties. The resulting film achieved a dielectric constant of 5.08 at 100 kHz and raised the maximum thermal temperature to 30 °C, demonstrating the synergistic enhancement of dielectric and thermal performance.

2 Experimental

2.1 Experimental Materials

4,4'-diaminodiphenyl ether (ODA, 99.5%), 4,4'-biphenyltetracarboxylic dianhydride (BPDA, 99.5%), 4,4 '-oxydiphthalic dianhydride (ODPA, 99.5%) were provided by Tianjin Zhongtai Material Technology Co., Ltd. (China); 3-Aminophenylboronic acid (3-ABBA, 98%)

was provided by Shanghai McLean Biochemical Technology Co., Ltd. (China); Toluene (analytical grade), N,N-dimethylformamide (DMF, analytical grade), N,N-Dimethylacetamide (DMAc, analytical grade) are provided by Sinopharm Chemical Reagent Co., Ltd. (China); Tetrahydrofuran (THF, 99.5%), ethanol (EtOH, 99.8%), dimethyl sulfoxide (DMSO, anhydrous solvent grade), dichloromethane (DCM, 99.5%), hydrochloric acid (HCl, analytical grade), and N-methyl pyrrolidone (NMP, 99.9%) were provided by Shanghai Aladdin Biochemical Technology Co., Ltd. (China).

2.2 Preparation of High Dielectric Constant Heat-Resistant TABO Crosslinked PI

(1) Preparation of TABO cross-linking agent

3-ABBA (3.10 g) and toluene (160 mL) were added to a 250 mL single-necked flask equipped with a Dean-Stark trap and a magnetic stir bar, and the resulting mixture was stirred at 300 rpm and refluxed for 12 h with an oil bath maintained at 120 °C. After centrifugation, the precipitate was washed three times with toluene until a pure white product was obtained. The product was then dried in a vacuum oven at 80 ℃ for 20 h to yield TABO. The synthetic route is outlined in Fig. 1(a).

(2) Preparation of crosslinked hard segment polyamic acid PAA-a

TABO (0.36 g) and DMAc (1.21 g) were added to a 5 mL two-necked flask and mechanically stirred until TABO was completely dissolved. BPDA (0.30 g) was then added in the flask and the mixture was reacted at room temperature for 5 h to obtain PAA-a. The synthesis steps are shown in Fig. 1(c).

(3) Preparation of soft segment polyamic acid PAA-b

ODA (3.70 g) and DMAc (21.00 g) were added to a 50 mL three-necked flask and

mechanically stirred until ODA was completely dissolved. ODPA (5.27 g) was then added in batches, and the mixture was reacted at room temperature under a nitrogen atmosphere for 5 h to obtain the PAA-b solution. The synthesis steps are shown in Fig. 1(b).

(4) Synthesis of soft-hard segmented PAA

PAA-a and PAA-b were transferred into a three-necked flask and stirred at 25 °C under a nitrogen atmosphere for 10 h to afford the soft-hard segmented PAA. A series of PAA solutions with varying proportions of BPDA in PAA-a and ODPA/ODA in PAA-b were prepared. The sample formulations were summarized in Table I.

(5) Synthesis of soft-hard segmented PI

The soft-hard segmented PAA solution was cast onto a glass plate using a 100 μm applicator and placed in a vacuum drying oven. The glass plate was heated at 160 ℃ under vacuum for 5 h to remove the solvent. The resulting film was then thermally imidized in a muffle furnace by heating at 200 °C for 1 h, followed by 330 °C for 30 min. After imidization, samples containing BPDA were designated as CO-X%-TABO, and those without BPDA designated as X%-TABO. The film preparation process is shown in Fig. 1(d).

The imidized films were soaked in water until the PI films detached from the glass substrate. The free-standing PI films were then dried in a vacuum oven at 100 ℃ for 10 h. The thickness of the dried films was approximately 30 μm.

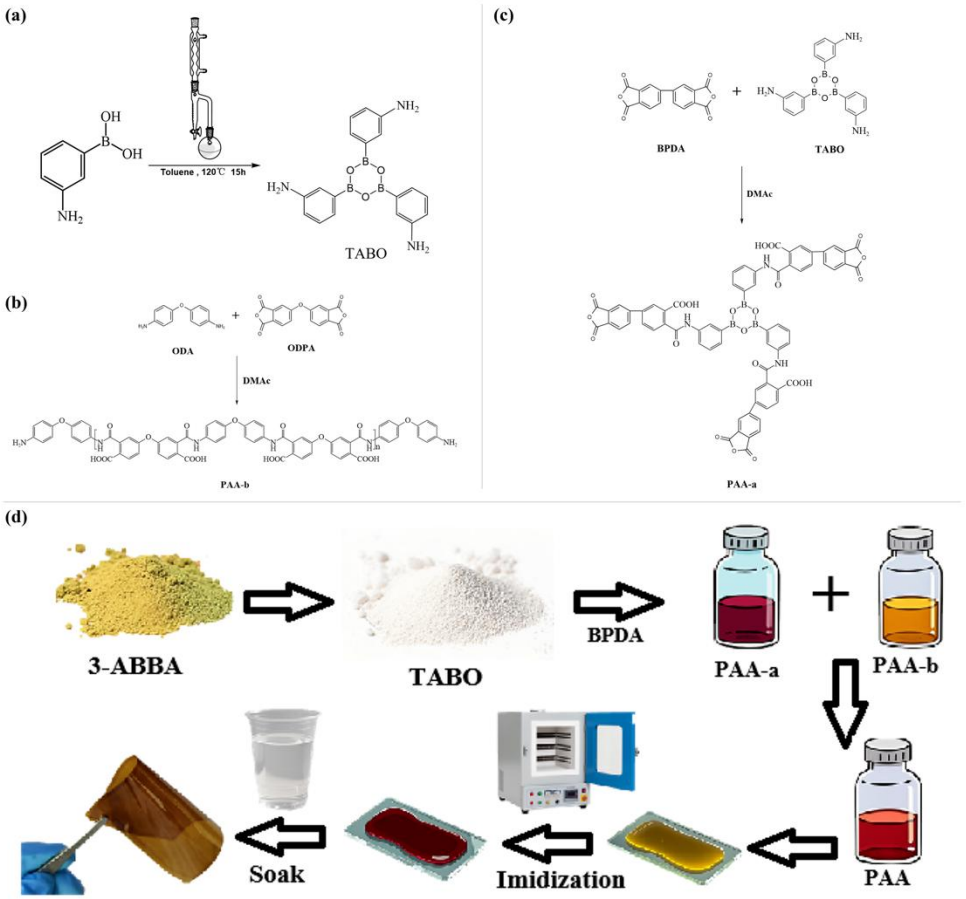


Fig. 1 Synthesis of (a)TABO, (b)PAA-b, (c)PAA-a and (d)Schematic diagram of preparation of modified PI

Table 1 Formulations of soft-hard segmented PAA

Sample	BPDA (mmol)	ODPA (mmol)	ODA (mmol)	TABO (mmol)
Pure	0	20	20.0	0
5%-TABO	0	30	28.5	1
7.5%-TABO	0	20	18.5	1
10%-TABO	0	15	13.5	1
CO-2.5%-TABO	3	57	58.5	1

CO-5%-TABO	3	27	28.5	1
CO-7.5%-TABO	3	17	18.5	1
CO-10%-TABO	3	12	13.5	1
CO-12.5%-TABO	3	9	10.5	1

2.3 Testing and Characterization

The structures of TABO and PI were tested by Fourier transform infrared spectrometer (FT-IR, Nicolet 6700, Thermo Fisher, USA). The PI film samples were analyzed in attenuated total reflection mode, whereas the powder residues obtained by calcining the PI films at 800 °C were analyzed in transmission mode over 400-4000 cm^{-1}, with a resolution of 2 cm^{-1} and 32 scans. Using deuterated DMSO as solvent, ^{11}B NMR was measured by superconducting nuclear magnetic resonance spectrometer (AVANCE NEO 600, Bruker, Switzerland). Thermogravimetric analysis (TGA) was performed on a thermogravimetric analyzer (TG209F1, Netzsch, Germany), the temperature was increased from 20 °C to 850 °C at a rate of 10 °C /min under a nitrogen atmosphere. The coefficient of thermal expansion (CTE) was carried out on a thermomechanical analyzer (TMA402F3, Netzsch, Germany) under a nitrogen atmosphere, traction was set at 30 mN and the heating rate was 5 °C /min in the range of 20-200 °C. The *Tg* was determined by differential scanning calorimetry (DSC Q2000, TA Instruments, USA) under a nitrogen atmosphere, the temperature was increased from 20 °C to 380 °C at a rate of 10 °C /min and subsequently cooled to 20 °C at a cooling rate of 5 °C /min. Thermal conductivity was measured by thermal conductivity meter (TC 3000E, XIATECH, China). The dielectric constant and loss were measured by LCR impedance analyzer (IM3533-

01, HIOKI, Japan), the test frequency was 1-200 kHz. The breakdown strength was tested by voltage breakdown tester (ZJC-50KV, AIETIMES, China) at a ramp rate of 1kV/s. Volumetric resistivity was determined using the volumetric surface resistivity tester (ZST-121, AIETIMES, China). The water contact angle was measured using a contact angle meter (JC2000DM, Zhongchen, China) employing the seat drop method, with deionized water as the liquid. Water absorption was determined by drying the PI films at 100 °C under vacuum for 24 h and recording their dry mass as W_1. The films were then immersed in deionized water for 24 h, surface-dried with filter paper, and weighed as W_2. Water absorption was calculated using equation (1), and the average of three measurements was reported.

$$\text{Water absorption} = (W_2 - W_1)/W_1 * 100\% \quad (1)$$

3 Results and Discussion

3.1 Structural Characterization

3.1.1 Infrared Spectrum Analysis of TABO

As shown in Fig. 2, both 3-ABBA and TABO exhibit a distinct absorption band at 715 cm^{-1}, corresponding to the bending vibration absorption peak of O-B-O bond. A new band appears at 765 cm^{-1} in the spectrum of TABO, corresponding to a characteristic vibrational mode of the six-membered boroxine ring[14]. This result suggests that the boroxine ring structure was formed during the reaction. The strong absorption band observed at 1360 cm^{-1} for both 3-ABBA and TABO is attributed to the stretching vibration of the B-O bonds. 3-ABBA exhibits a broad and intense absorption band near 3260 cm^{-1}, which is associated with the stretching vibration of the hydroxyl groups in the boronic acid moieties. In contrast, only a weak band remains at this position in the spectrum of TABO, indicating that most of the boronic acid groups underwent dehydration–condensation to form boroxine rings. The residual band may be attributed to the partial hydrolysis of the product upon exposure to moisture in air, which regenerated a small number of B-OH groups. In addition, both 3-ABBA and TABO display a distinct band near 3390 cm^{-1}, corresponding to the N-H stretching vibration of the amino groups, indicating that the amino functionality was retained in TABO. To sum up, the appearance of the characteristic boroxine-ring band at 765 cm^{-1}, together with the significant weakening of the B-OH stretching band near 3260 cm^{-1}, confirms that the dehydration condensation reaction of 3-ABBA occurred successfully and supports the formation of the desired boroxine ring structure in TABO.

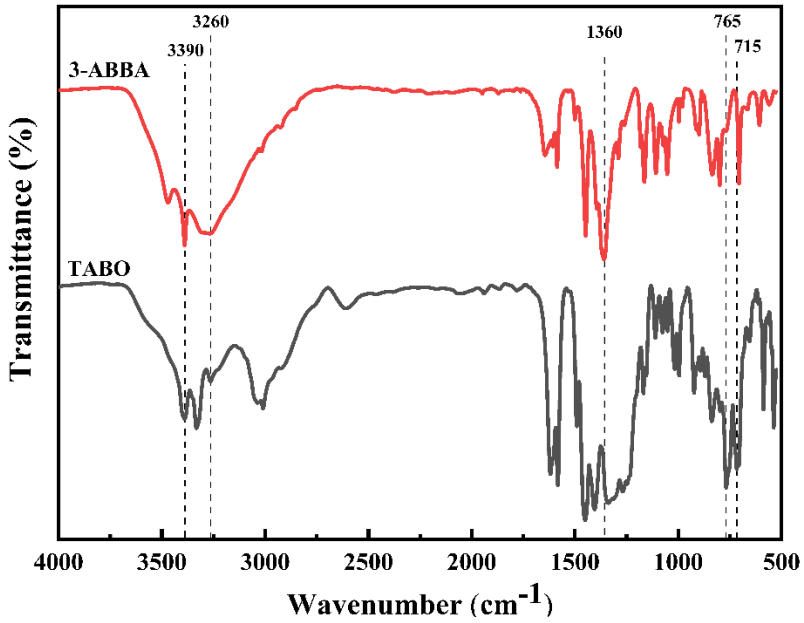


Fig. 2 FT-IR spectra of 3-ABBA and TABO

3.1.2 Infrared Spectrum Analysis of PI Modified by TABO

As shown in Fig. 3, the absorption bands at 1710 cm^{-1} and 1775 cm^{-1} are assigned to the symmetric and asymmetric stretching vibrations of C=O in the imide rings, respectively. The band at 1368 cm^{-1} is attributed to the stretching vibration of the imide C-N bond. while the band at 1500 cm^{-1} corresponds to the skeletal stretching vibration of the aromatic rings. These characteristic absorption bands confirm the formation of the polyimide structure[15]. In the FTIR spectrum of the 10%-TABO sample, the absorption peak at 715 and 765 cm^{-1}, which attributed to the characteristic absorption of the boroxine ring, are clearly observed, confirming the chemical incorporation of TABO into the PI chains.

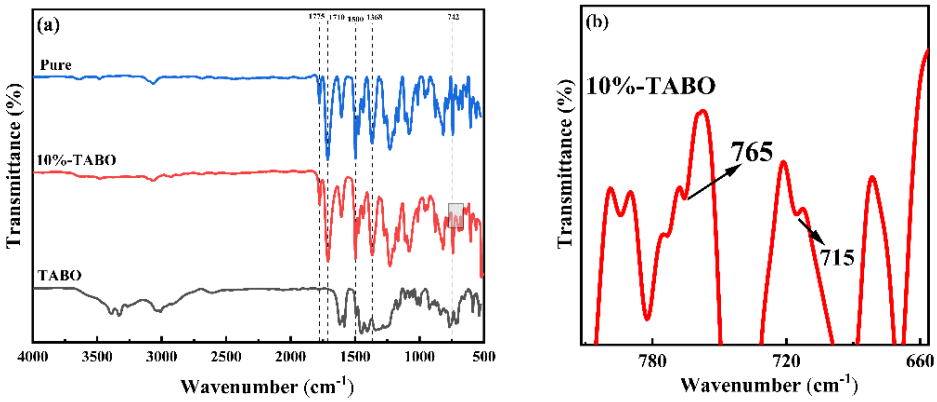


Fig. 3 FT-IR spectra of (a) Pure, 10%-TABO, and TABO and (b) enlarged spectrum of the 10%-TABO sample in the range of 650-800 cm^{-1}.

3.1.3 TABO NMR Characterization

The ^{11}B NMR spectra of 3-ABBA and TABO are shown in Fig. 4. The ^{11}B NMR signal shifted from 27.52 ppm for 3-ABBA to 28.17 ppm for TABO, indicating a downfield shift. This shift is attributed to the dehydration condensation of the acyclic boronic acid groups to form a cyclic boroxine ring structure[16]. These results confirm the successful synthesis of TABO.

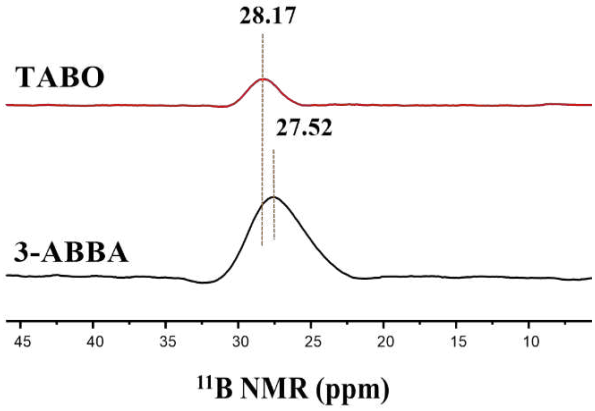


Fig. 4 NMR spectra of the TABO and 3-ABBA

3.2 Thermal Performance Analysis

3.2.1 Thermogravimetric Analysis

Fig. 5 (a) presents the thermogravimetric and derivative thermogravimetric curves of

TABO-modified PI films measured in air. The corresponding thermal decomposition parameters are summarized in Table II. With increasing the molar ratio of TABO to ODA, the 5%, 10% weight-loss temperature ($T_{5\%}$, $T_{10\%}$) of the PI series samples increased progressively. In particular, the $T_{5\%}$ values of the TABO-modified PI films exceeded 500 °C, higher than 491 °C for the pure PI. This enhancement can be attributed to the introduction of rigid and thermally stable boroxine rings by TABO. In addition, the multifunctional TABO units serve as effective cross-linking points, restricting the motion of the PI molecular chains and suppressing thermal decomposition at elevated temperatures. At higher temperatures, the boron-containing structures also promote the formation of a protective boron oxide-rich layer, which further improves the thermal stability of the PI films.

3.2.2 Glass Transition Temperature

The DSC cooling curves of TABO-modified PI films are shown in Fig. 5 (b). As the molar ratio of TABO to ODA increases, the *Tg* of the PI films increased progressively. Near the glass transition temperature, the polymer segments acquire sufficient thermal energy to undergo cooperative motion. However, the rigid and thermally stable six-membered boroxine rings in TABO act as rigid junctions that constrain the surrounding PI chain segments. Consequently, the rotational and translational motions of the chains are restricted, and a higher temperature is required to activate segmental motion, resulting in an increase in the *Tg* of the PI films.

3.2.3 Coefficient of Thermal Expansion

Figure 5(c) presents the coefficients of thermal expansion of the TABO-modified PI films. Pure PI exhibited a CTE of 62.2 ppm K^{-1}, and the CTE decreased progressively with increasing the molar ratio of TABO to ODA. This reduction can be attributed primarily to the increased

effective cross-linking density and structural rigidity introduced by TABO. As a multifunctional monomer, TABO introduces additional junction points into the polymer structure, thereby restricting chain-segment mobility and reducing thermally induced dimensional changes. Moreover, the rigid six-membered boroxine rings further enhance the overall rigidity of the PI structure and constrain local segmental motion. Consequently, the thermal expansion of the PI films is effectively suppressed, resulting in lower CTE values.

3.2.4 Thermal Conductivity

Fig. 5(d) presents the thermal conductivities of the PI films with different molar of TABO to ODA. The thermal conductivity increased from 0.1068 W m^{-1} K^{-1} for pure PI to 0.2156 W m^{-1} K^{-1} for the film of CO-10%-TABO, corresponding to an approximately 2.02-fold increase. Because PI is an electrically insulating polymer, heat is transported primarily through molecular vibrations, or phonons[17]. Phonon transport is strongly affected by chain disorder, free volume, and structural defects, all of which can increase phonon scattering. The incorporation of TABO improves the thermal conductivity of the PI films, because the rigid boroxine rings and strong B-O bonds increase the structural rigidity of the polymer, and provide relatively efficient pathways for vibrational energy transfer. In addition, the multifunctional TABO units increase the effective intermolecular cross-linking density and reduce the free volume of the PI. These effects restrict chain-segment motion, improve the local packing of the polymer chains, and reduce phonon scattering. Consequently, the thermal conductivity of the TABO-modified PI films increases with increasing the molar ratio of TABO to ODA.

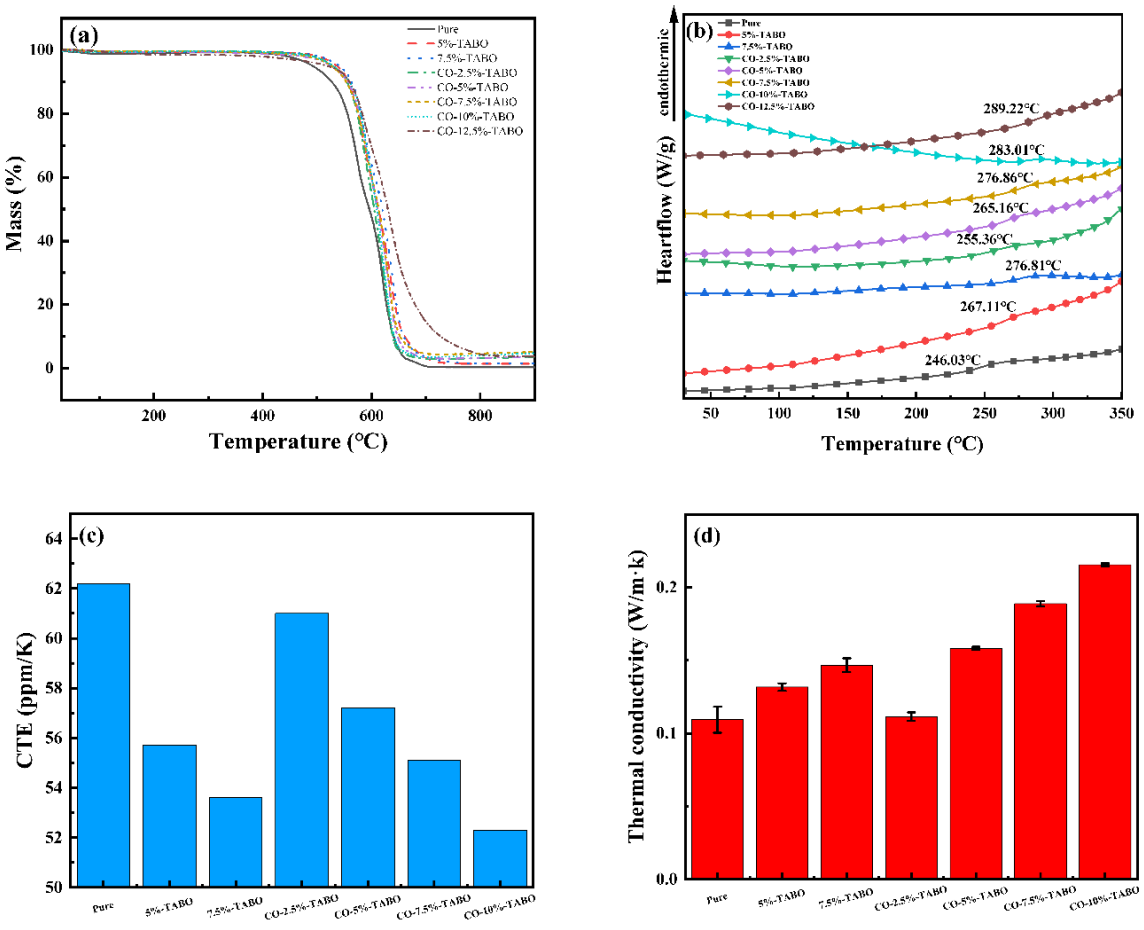


Fig. 5 Thermal properties of different component samples:

(a) thermogravimetric (TG) and derivative thermogravimetric (DTG) curves; (b) differential scanning calorimetry (DSC) curves; (c) coefficient of thermal expansion (CTE); and (d) thermal conductivity.

Table 2 Thermal performance data of TABO modified PI

	Thermogravimetric properties			
	$T_{5\%}$ (°C)	$T_{10\%}$ (°C)	T_{max} (°C)	Residual mass at 800 (%)
Pure	491	527	600	0.29
5%-TABO	529	557	610	1.38

7.5%-TABO	540	563	615	1.52
10%-TABO	553	571	630	2.82
CO-2.5%-TABO	529	554	620	3.15
CO-5%-TABO	525	555	626	3.21
CO-7.5%-TABO	526	553	626	4.15
CO-10%-TABO	529	559	630	4.08
CO-12.5%-TABO	518	559	636	4.34

3.3 Electrical Performance Analysis

3.3.1 Dielectric Properties

The dielectric constant is directly related to a material's ability to store charge, while dielectric loss factor characterizes the energy loss of the material in an alternating electric field. Fig. 6 (a) shows the frequency dependence of the dielectric constant of the TABO-modified PI samples. As the molar ratio of TABO to ODA increased, the dielectric constant of modified PI films gradually increased. At 100 kHz, the CO-10%-TABO sample exhibited a dielectric constant of 5.08, compared with 3.21 for pure PI, corresponding to an increase of approximately 58.3%. The dielectric constants of the soft-hard segmented PI films CO-5%-TABO and CO-7.5%-TABO were 4.02 and 4.34, respectively. These values surpass those of the corresponding reference samples with the same molar ratio of TABO, namely 3.98 for 5%-TABO and 4.25 for 7.5%-TABO. The enhanced dielectric performance can be attributed to the

more homogeneous three-dimensional network formed by the reaction between the soft and hard segments. This uniformly distributed cross-linking structure reduces the free volume and promotes denser packing of the polymer chains. Moreover, the highly polar B-O bonds introduced during crosslinking enhance dipolar and interfacial polarization under an applied electric field, thereby improving the dielectric performance of the material.[18]

Fig. 6(b) shows the frequency dependence of the dielectric loss factor of the TABO-modified PI samples. The dielectric loss generally increases with increasing molar ratio of TABO to ODA. The reason is that the high content of B-O bonds significantly increases the density of polar groups in the material, leading to dipole polarization and enhanced local vibration energy dissipation. In addition, excessive cross-linking may introduce structural defects such as microcracks, further amplifying local polarization relaxation.

3.3.2 Breakdown Strength

Fig. 6(c) shows the Weibull distribution of the breakdown strength of TABO-modified PI samples. The breakdown strength showed a progressive decrease with increasing molar ratio of TABO to ODA. The reason is that the three-dimensional cross-linked network introduced by TABO significantly disrupts the regularity of PI molecular chains, and the rigid biphenyl structure of ODPA-ODA in the linear main chain is oriented due to the distortion of cross-linking points[19]. At the same molar ratio of TABO to ODA, the block-copolymerized PI samples exhibit higher breakdown strengths than the corresponding non-block samples. In the stepwise synthesis, TABO is first reacted with BPDA to form the rigid PAA-a segment, which is subsequently combined with the ODPA/ODA-derived flexible PAA-b segment. Compared with the non-block synthesis route, this controlled reaction sequence promote a more uniform

distribution of cross-linking sites and reduce local structural heterogeneity. Consequently, electric-field distortion and charge accumulation may be alleviated, partially mitigating the adverse effect of TABO incorporation on the breakdown strength.

3.3.3 Volume Resistivity

Fig. 6(d) shows the volume resistivity of TABO-modified PI. The pure PI exhibits a volume resistivity of 6.48×10^{15} Ω·cm, and the volume resistivity of all TABO modified PI is higher than 10^{17} Ω·cm, indicating excellent electrical insulating properties. With the TABO molar ratio of TABO to ODA increased, the volume resistivity of modified PI film also increased. The volume resistivity of the CO-10%-TABO film reached 5.3×10^{18} Ω·cm, approximately 818 times that of pure PI. The increase can be attributed to the incorporation of TABO as a cross-linking agent, which forms a highly cross-linked network that restricts segmental motion and promotes more compact molecular-chain packing. This structure suppresses charge-carrier transport, thereby improving the volume resistivity of the PI films. In addition, the tightly cross-linked network also promotes denser molecular-chain packing and reduce local structural defects. These results demonstrate that the TABO-modified PI films retain excellent electrical insulation properties and show potential for electronic packaging and electrical insulation applications.

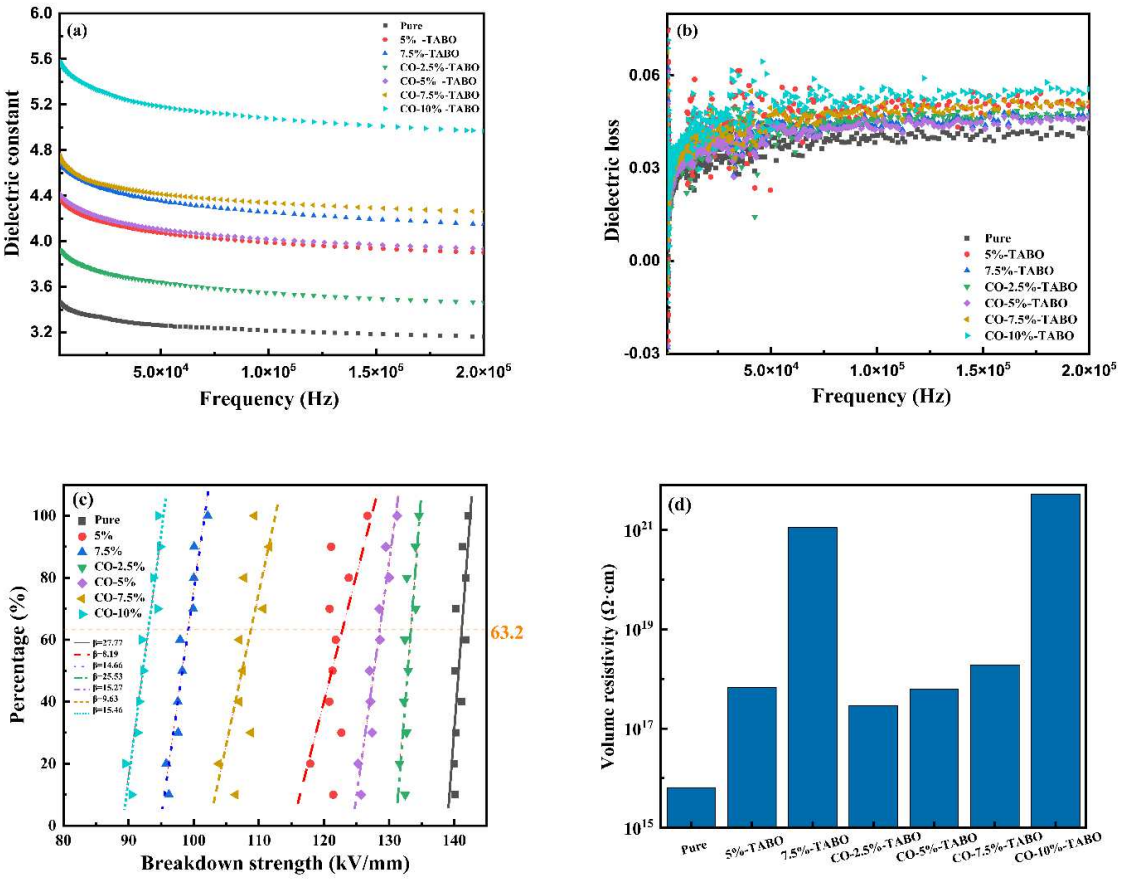


Fig. 6 Dielectric properties of different component samples: (a) Dielectric constant; (b) Dielectric loss; (c) Distribution diagram of breakdown strength; (d) Volume resistivity

3.4 Water Contact Angle and Water Absorption Rate

For dielectric materials used in humid environments, surface wettability is an important factor affecting their electrical insulation and dielectric stability. Fig. 7 shows the water contact-angle images of PI film different component. The pure PI film exhibits a water contact angle of 81.03°. With the molar ratio of TABO to ODA increased, the water contact angle gradually increased, reaching 89.11° in the CO-10%-TABO film. This increase indicates reduced surface wettability and suggests that the incorporation of TABO improves the moisture resistance of the PI films.

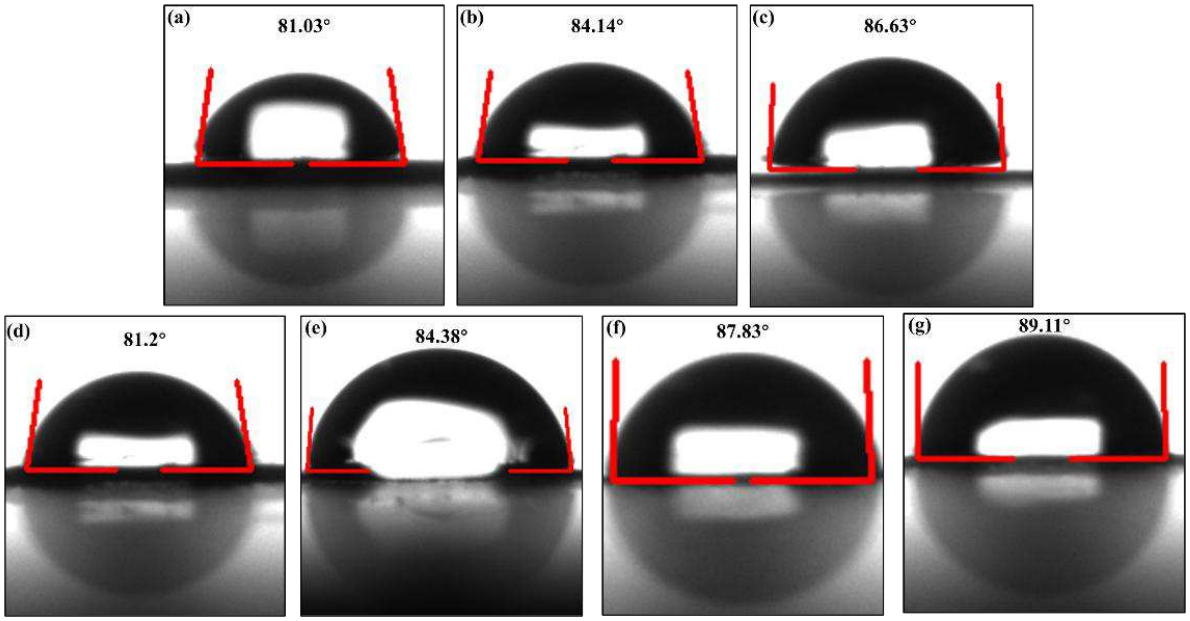


Fig. 7 Surface contact angle of different component samples:

(a)PI-Pure; (b)5%-TABO; (c)7.5%-TABO; (d)CO-2.5%-TABO; (e)CO-5%-TABO; (f)CO-7.5%-TABO; (g)CO-10%-TABO

The water absorption values of the PI films are summarized in Table III. The water absorption rate of pure PI is 3.86%. As the molar ratio of TABO to ODA increased, the water absorption rate of modified PI film gradually decreased. The water absorption in the CO-10%-TABO film, decreases to 3.11%, representing a reduction of approximately 19.4%. Together with the water contact-angle results, these results indicated that the incorporation of TABO reduced water uptake and improved the moisture resistance of the PI films.

Table 3 water absorption of different component samples

Sample	Water absorption (%)
Pure	3.86
5%-TABO	3.36

7.5%-TABO	3.21
CO-2.5%-TABO	3.51
CO-5%-TABO	3.32
CO-7.5%-TABO	3.25
CO-10%-TABO	3.11

3.5 Mechanical Properties

Fig. 8(a) presents the stress-strain curve of the TABO-modified PI films, and Fig. 8(b) summarizes their elongation at break and tensile strength. As the molar ratio of TABO to ODA increased, the tensile strength initially increased and then decreased, whereas the elongation at break decreased progressively. For TABO-to-ODA molar ratios of 2:27, 2:37, and 2:57, the formation of a cross-linked network restricted molecular-chain slippage and improved load transfer between polymer chains, thereby enhancing tensile strength. The rigid boroxine rings introduced by TABO have further contributed to this improvement. However, an excessively high cross-linking density severely restricted segmental mobility and plastic deformation, thereby reducing the flexibility and ductility of the films. It also has caused local stress concentrations, facilitating premature fracture. At TABO-to-ODA molar ratios above 2:57, the film became more brittle, resulting in decreases in both tensile strength and elongation at break.

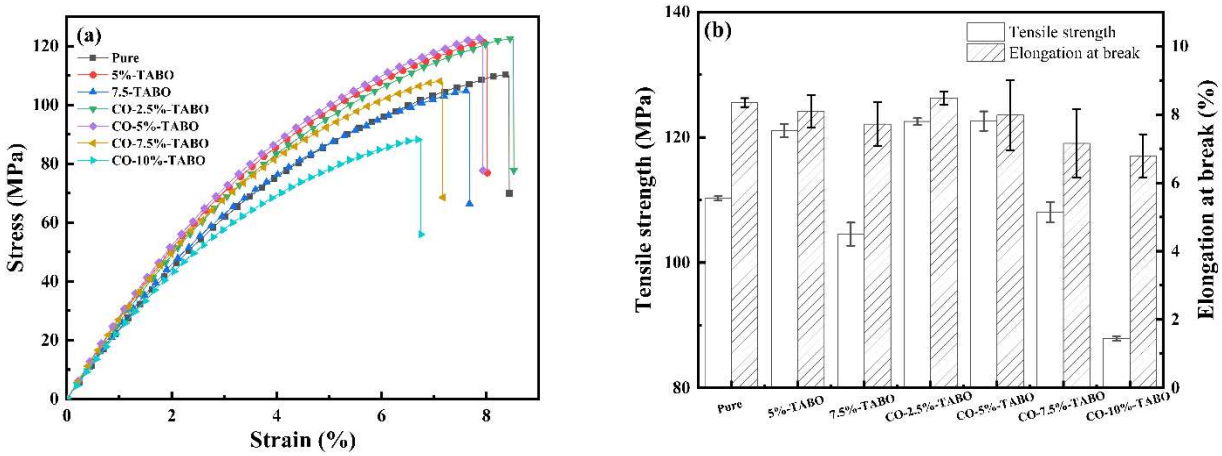


Fig. 8 Stress-strain curve(a) and fracture elongation and tensile strength(b) of TABO modified PI

4 Conclusion

In this study, TABO was synthesized through the dehydration condensation of 3-ABBA. A series of TABO-modified PI films were prepared via stepwise soft-hard segmented polycondensation, followed by solution casting and thermal imidization. The results showed that the incorporation of TABO and the formation of a cross-linked network effectively restricted molecular-chain motion and reduced energy dissipation, thereby improving the thermal stability, dielectric properties, and mechanical performance of the PI films. With the TABO-to-ODA molar ratio increased, the thermal stability generally improved and the dielectric constant gradually increased, whereas the mechanical properties first increased and then decreased, indicating that excessive cross-linking could embrittle the films. In conclusion, the TABO-modified PI films exhibited superior comprehensive performance compared with pure PI. The CO-10%-TABO film achieved a dielectric constant of 5.08 at 100 kHz and a maximum decomposition rate temperature of 630 °C. These findings highlight the potential of the resulting PI films for applications in high-energy-density capacitors.

Acknowledgments

The analysis work of this article was partially carried out at the Instrumental Analysis Center, Hefei University of Technology.

Author contributions

Shengjie Ge: investigation, data collection, writing, editing of the manuscript. Xiang Zhang: supervision, project administration, resources. Fengmei Ren: formal analysis, investigation, validation. Haihong Ma: validation and writing review editing. Zhengfa Zhou: reviewed the manuscript. Weibing Xu: visualization and investigation.

Disclosure statement

The authors declare that they have no known competing financial interests or personal rela-tionships that could have appeared to influence the work reported in this paper.

Data availability

Data will be made available on request.

5 References

[1] H. Tao, M. Yan, L. Zhang, Z. Zou, B. Han, H. Dong, B. ZhuX. Li, Progress in preparation, processing, and application of high dielectric polypropylene matrix composite materials. Polym. Compos. **45**, 4819 (2024). https://doi.org/10.1002/pc.28111

[2] L. Zhou, N. Song, X. Wang, L. Wei, H. CaiT. Ji, Analysis on dielectric loss characteristics of polyvinylidene fluoride and its composites. Journal of Materials Science. Materials in Electronics **32**, 26268 (2021). https://doi.org/10.1007/s10854-021-06893-4

[3] Y. Tang, H. Yao, W. Xu, L. Zhu, Y. ZhangZ. Jiang, Side-chain-type high dielectric-constant dipolar polyimides with temperature resistance. Macromol. Rapid Commun. **44**, 2200639 (2023). https://doi.org/10.1002/marc.202200639

[4] L. Ren, H. Li, Z. Xie, D. Ai, Y. Zhou, Y. Liu, S. Zhang, L. Yang, X. ZhaoZ. Peng, High-temperature high-energy-density dielectric polymer nanocomposites utilizing inorganic core–shell nanostructured nanofillers. Adv. Energy Mater. **11**, 2101297 (2021). https://doi.org/10.1002/aenm.202101297

[5] R. Xu, J. Ma, R. Zhou, H. Sun, D. XuZ. Zeng, Black phosphorus nanoflakes/polyimide composite films with excellent dielectric and mechanical properties. Journal of Materials Science: Materials in Electronics **31**, 3303 (2020). https://doi.org/10.1007/s10854-020-02878-x

[6] D. Wu, X. Zhao, X. Li, J. DongQ. Zhang, Polyimide film containing sulfone groups with high dielectric properties. Polymer **256**, 125221 (2022). https://doi.org/10.1016/j.polymer.2022.125221

[7] H. Tong, J. Fu, A. Aftab, T. Fan, Y. HouJ. Xu, Sulfonyl-containing polyimide dielectrics with advanced heat resistance and dielectric properties for high-temperature capacitor applications. Macromolecular Materials & Engineering **304**, 1800709 (2019). https://doi.org/10.1002/mame.201800709

[8] T. Zhu, Q. Yu, W. Zheng, R. Bei, W. Wang, M. Wu, S. Liu, Z. Chi, Y. ZhangJ. Xu, Intrinsic high-k-low-loss dielectric polyimides containing ortho-position aromatic nitrile moieties: Reconsideration on clausius-mossotti equation. Polym Chem-Uk **12**, 2481 (2021). https://doi.org/10.1039/d1py00084e

[9] L. Chen, Y. Ding, T. Yang, C. WanH. Hou, Synthesis and properties of a high dielectric constant copolymer of copper phthalocyanine oligomer grafted to amino-capped polyimide. J. Mater. Chem. C **5**, 8371 (2017). https://doi.org/10.1039/c7tc03169f

[10] D. Fang, K. Yao, Y. Ding, P. LiH. Hou, High dielectric polyimide composite film filled with a heat-resistant organic salt. Compos. Commun. **14**, 29 (2019). https://doi.org/10.1016/j.coco.2019.05.008

[11] G. Mierzwa, A.J. Gordon, Z. LatajkaS. Berski, On the multiple b-o bonding using the topological analysis of electron localisation function (elf). Computational & theoretical chemistry **1053**, 130 (2015). https://doi.org/10.1016/j.comptc.2014.10.003

[12] T. Wu, D. Wang, Q. Wang, X. Chen, J. DingX. Yan, Study on network structure and heat resistance in air of boron-modified phenolic resin aerogel. Polymers **17**, 860 (2025). https://doi.org/10.3390/polym17070860

[13] P. Wang, Z. Wang, W. CaoJ. Zhu, Facile preparation of a transparent, self-healing, and recyclable polysiloxane elastomer based on a dynamic imine and boroxine bond. Polymers **16**, 1262 (2024). https://doi.org/10.3390/polym16091262

[14] R. L, L. CQ. T, Preparation of boroxine-based self-healing polyurethane with repeatable adhesive property under mild conditions. Mater. Today Chem. **26**, 101126 (2022). https://doi.org/10.1016/j.mtchem.2022.101126

[15] T. Yang, W. Xu, X. PengH. Hou, Crown ether-containing polyimides with high dielectric constant. RSC Adv. **7**, 23309 (2017). https://doi.org/10.1039/c7ra03891g

[16] X. Li, Y. Zhang, Z. Shi, D. Wang, H. Yang, Y. Zhang, H. Qin, W. Lu, J. ChenY. Li, Water-stable boroxine structure with dynamic covalent bonds. Nat. Commun. **15**, 1207 (2024). https://doi.org/10.1038/s41467-024-45464-z

[17] N. Burger, A. Laachachi, M. Ferriol, M. Lutz, V. ToniazzoD. Ruch, Review of thermal conductivity in composites : Mechanisms, parameters and theory. Prog. Polym. Sci. **61**, 1 (2016). https://doi.org/10.1016/j.progpolymsci.2016.05.001

[18] T. Zhang, C. Wang, G. Liu, C. Yao, X. Zhang, C. ZhangQ. Chi, High thermal conductivity and low dielectric loss of three-dimensional boron nitride nanosheets/epoxy composites. Compos. Commun. **50**, 102007 (2024). https://doi.org/10.1016/j.coco.2024.102007

[19] Y. Dong, Z. Wang, S. Huo, J. LinS. He, Improved dielectric breakdown strength of polyimide by incorporating polydopamine-coated graphitic carbon nitride. Polymers **14**, 385 (2022). https://doi.org/10.3390/polym14030385